A Model for Air–Sea Interaction Bulk Coefficient over a Warm Mature Sea under Strong Wind

NAOTO KIHARA AND HIROMARU HIRAKUCHI

Civil Engineering Research Laboratory, Central Research Institute of Electric Power Industry, Abiko, Abiko-shi, Chiba, Japan

(Manuscript received 24 April 2007, in final form 12 October 2007)

ABSTRACT

A boundary layer model for evaluating sensible and latent heat fluxes over a mature sea accounting for sea spray effects at wind speeds of up to 28 m s^{-1} is presented. Heat exchange across the ocean surface controls the development of tropical cyclones, and Emanuel's theory suggests that the ratio of the exchange coefficient of total enthalpy to the drag coefficient should be greater than 0.75 to maintain the intensity of tropical cyclones. However, traditional bulk algorithms predict a monotonic decrease in this ratio with increasing wind speed, giving a value of less than 0.5 under tropical cyclone conditions. The present model describes a decrease in the ratio with increasing wind speed under weak to moderate winds (<20 m s^{-1}), and a plateau at approximately 0.7 under strong winds (>20 m s^{-1}).

1. Introduction

The development of tropical cyclones is governed by heat exchange between the air and the sea. Emanuel (1986) proposed a simple energy balance model for tropical cyclones in which the inner region of the tropical cyclone plays a role similar to that of a Carnot heat engine, extracting latent and sensible heat from the ocean and transferring that heat outward to overcome frictional dissipation in the boundary layer at large radii. Thus, extracting heat is seen as essential to maintain the intensity of a tropical cyclone.

In meteorological models, heat transfer from the sea surface is generally estimated using bulk algorithms, which have been investigated extensively using large datasets of observations. Fairall et al. (1996) proposed a method for flux estimation using bulk variables obtained by the Tropical Ocean and Global Atmosphere Coupled Ocean–Atmosphere Response Experiment (TOGA COARE) for weak to moderate winds ($0.5 \le u_{10} \le 10$ m s^{-1}). It was shown that the exchange coefficient for latent heat flux corrected for neutral stratification is an approximately constant value of 1.11×10^{-3}, decreasing slightly with wind speed. DeCosmo et al. (1996) developed a bulk algorithm using the dataset of the Humidity Exchange over the Sea (HEXOS) program. The HEXOS data were collected near the Dutch coast at wind speeds of up to 18 m s^{-1} and are thus affected by sea spray due to shallow wave breaking. The exchange coefficients for sensible heat (C_T) and latent heat (C_q) under neutral stratification determined in the study of DeCosmo et al. (1996) are $C_T = (1.12 \pm 0.24) \times 10^{-3}$ and $C_q = (1.14 \pm 0.35) \times 10^{-3}$. In short, based on the large datasets collected under both of these programs (TOGA COARE and HEXOS), C_T and C_q appear to take approximately constant values of 1.1×10^{-3} for the wind speed range of $0.5 \le u_{10} \le 18$ m s^{-1}, although the data exhibit considerable scatter. However, as there have been relatively few observations of latent heat flux over the ocean under stronger wind conditions, it remains unknown whether it is valid to extrapolate these bulk algorithms to stronger winds.

Emanuel (1995a) doubted that the bulk algorithms could be reasonably extended to tropical cyclone conditions, and he conducted a theoretical study of the effect of the exchange coefficient of total enthalpy on tropical cyclone intensity using a simple balance model (Emanuel 1995b) and a nonhydrostatic convection model (Rotunno and Emanuel 1987). It was thus shown that tropical cyclone intensity is dependent on the ratio of the exchange coefficient of total enthalpy (C_G) to the drag coefficient (C_D), leading to the conclusion that the ratio C_G/C_D in the strong wind region of intense storms

Corresponding author address: Naoto Kihara, Civil Engineering Research Laboratory, Central Research Institute of Electric Power Industry, 1646 Abiko, Abiko-shi, Chiba 270-1194, Japan.
E-mail: kihara@criepi.denken.or.jp

DOI: 10.1175/2007JPO3828.1

must be greater than 0.75 to maintain the intensity of a tropical cyclone. Here, the total enthalpy G is defined as

$$G \equiv c_{\rm pa}T + L_E q, \tag{1}$$

where T is the temperature, q is the specific humidity, $c_{\rm pa}$ is the specific heat at a constant pressure of air, and L_E is the latent heat of evaporation of water, respectively. The exchange coefficient of total enthalpy C_G is defined as

$$\begin{aligned} H_G &\equiv H_S^{\rm tot} + H_L^{\rm tot} \\ &= \rho_a C_G[c_{\rm pa}(T_w - T_{10}) + L_E(q_w - q_{10})]u_{10}, \end{aligned} \tag{2}$$

where H_G is the total enthalpy flux, $H_S^{\rm tot}$ is the total sensible heat flux, $H_L^{\rm tot}$ is the total latent heat flux, ρ_a is the density of air, T_{10} is the temperature at a 10-m height, T_w is the sea surface temperature, q_{10} is the specific humidity at a 10-m height, and q_w is the saturation-specific humidity at the sea surface temperature. In general, C_D increases with wind speed (e.g., Large and Pond 1981). Extrapolating the results of the large programs (i.e., TOGA COARE and HEXOS) to the stronger winds ($u_{10} > 18$ m s^{-1}), both the exchange coefficients of sensible heat and latent heat become approximately constant at 1.1×10^{-3} and are independent of wind speed. Thus, C_G becomes approximately constant at 1.1×10^{-3} from Eq. (2). Then, the bulk algorithms predict that the ratio C_G/C_D will decrease with increasing wind speed and become less than 0.75 at $u_{10} > 20$ m s^{-1}. Even using the recent findings that the drag coefficient does not increase with wind speed for strong winds ($u_{10} > 33$ m s^{-1}) and holds a constant value of about 2.5×10^{-3} (Powell et al. 2003; Donelan et al. 2004), the ratio C_G/C_D becomes 0.44 at $u_{10} > 33$ m s^{-1}, for which Emanuel's theory predicts that the central surface pressure of a steady tropical cyclone will be greater than 980 hPa. In short, the exchange coefficient of total enthalpy must increase with wind speed under tropical cyclone conditions if Emanuel's model is correct.

Sea spray has been considered a likely factor that may resolve this discrepancy (Andreas and Emanuel 2001). Under strong wind, sea spray is generated by wave breaking, and the droplets of sea spray drifting in the atmosphere continue to transfer sensible heat to the ambient atmosphere until the droplet temperature reaches the wet-bulb temperature, at which time the droplet evaporates and generates latent heat by absorbing sensible heat from the atmosphere. This heat exchange between sea spray droplets and the atmosphere mainly occurs within a droplet evaporation layer (DEL).

The possible effect of sea spray on tropical cyclone intensity has been investigated by a number of groups. For example, using a coupled ocean–atmosphere model of a tropical cyclone, Kepert et al. (1999) concluded that although sea spray had little effect on the total enthalpy flux, it could increase storm intensity by cooling and moistening the boundary layer. Wang et al. (2001) came to a similar conclusion using the parameterization of Fairall et al. (1994), but also showed that sea spray contributes directly to the total enthalpy flux if the parameterization of Andreas and DeCosmo (1999) is assumed. These early studies thus suggest that sea spray may increase the total enthalpy flux from the ocean and also cool and moisten the boundary layer.

Sensible and latent heat are transferred by turbulence in the airflow. As the airflow immediately above the ocean is disturbed by ocean waves, forming a wave boundary layer (WBL), the turbulent transfer in the WBL must be affected by ocean waves (Makin and Mastenbroek 1996; Makin 1999). A number of WBL models have been proposed to predict the drag coefficient (e.g., Janssen 1989; Makin and Kudryavtsev 1999), and most consider momentum conservation in the WBL. These studies indicate that turbulent momentum flux in the WBL is reduced by wave-induced momentum flux related to periodic airflow perturbations generated by ocean waves. Recently, Hara and Belcher (2004) proposed a WBL model based on the conservation of both momentum and kinetic energy over ocean waves, and Moon et al. (2004a) combined the model of Hara and Belcher with a wavenumber spectrum calculated by the WAVEWATCH III wave model (Tolman 2002) to investigate the momentum exchange process for young and mature seas. Application of that model under conditions of hurricane wind forcing (Moon et al. 2004b,c) revealed the same plateauing of the drag coefficient at $u_{10} \geq 35$ m s^{-1} as indicated by the observations of Powell et al. (2003). This result suggests that it may soon be possible to solve many of the unanswered questions related to transfer mechanisms in the boundary layer over the ocean.

Moon et al. (2007) proposed a new roughness length of z_0 for momentum, based on a sequence of their results using the WBL model (Moon et al. 2004b,c) under conditions of hurricane wind forcing, and they investigated the effects of the use of the new roughness length for momentum on the intensity of tropical cyclones. They showed that the ratio C_G/C_D lies in the range of 0.7–1.4 and increases as wind speed increases, by using the relation of

$$C_D = \kappa^2\left(\ln\frac{10}{z_0}\right)^{-2}, \tag{3}$$

$$C_G = \kappa^2\left(\ln\frac{10}{z_0}\right)^{-1}\left(\ln\frac{10}{z_T}\right)^{-1}, \tag{4}$$

where κ is the von Kármán constant. However, because they focused on the impact of the new roughness length z_0 for momentum, they simply used a Charnock-type roughness length (Charnock 1955) for temperature and humidity:

$$z_T = 0.0185\frac{g}{u_*^2}. \tag{5}$$

In the case that the bulk algorithm of Zeng et al. (1998), which is based on the results of the abovementioned large programs, is adopted for the estimation of z_T [shown in Eq. (49)], the ratio C_G/C_D using z_0 of Moon et al. (2007) monotonically decreases as wind speed increases, and the ratio becomes less than 0.5 at $u_{10} >$ 35 m s^{-1}, as also shown by the traditional bulk algorithms. In their conclusion, they pointed out the need for further studies of heat transfer in strong wind conditions.

Makin and Mastenbroek (1996) and Makin (1999) evaluated heat transfer in the WBL using their WBL model.

In the present study, a boundary layer model for evaluating sensible and latent heat fluxes including sea spray–mediated heat fluxes over a mature sea is developed. The WBL model of Hara and Belcher (2004) is adopted as a basis, the wavenumber spectrum for mature sea presented by Elfouhaily et al. (1997) is used for the low-wavenumber regime, and that proposed by Hara and Belcher (2002) is used for the high-wavenumber regime. Using the information on the airflow structure obtained from the WBL model, turbulent heat transfer in the WBL is calculated using the approach of Makin and Mastenbroek (1996). The sea spray–mediated heat flux in the DEL is incorporated by introducing the parameterization of Fairall et al. (1994). The results of the developed model are used to evaluate the increase in total enthalpy under strong wind conditions.

Reduction of momentum flux in the airflow due to sea spray is not considered. The momentum of airflow is extracted by the spray droplets drifting in the atmosphere due to the acceleration of the droplets in the direction of the wind. Wu (1973) found that such momentum exchange is negligible under moderate winds, and Andreas and Emanuel (2001) showed that the contribution of this momentum exchange is three orders of magnitude less than the interfacial stress for moderate winds, although the interfacial and spray stresses become comparable for strong winds ($u_* \geq 3$ m s^{-1}). The friction velocity ($u_* = 3$ m s^{-1}) corresponds to $u_{10} = 60$ m s^{-1} when $C_D = 0.0025$. In the present study, heat transfer is investigated at wind speeds of up to $u_{10} = 28$ m s^{-1}, at which the top of DEL reaches $z = 10$ m (the reference height of bulk variables). Thus, the sea spray–mediated momentum flux is considered to be negligible in the present study.

This paper is organized as follows: in section 2, the model and solving procedures are introduced. In section 3, the sensible and latent heat transfer over a mature sea without sea spray effects is evaluated, and the influence of sea spray is then discussed. The growth of the exchange coefficient of total enthalpy under tropical storm conditions is then evaluated. The main results of the present study and future work are finally presented in section 4.

2. Model description

a. Wave boundary layer model

The momentum flux over the ocean waves is estimated by applying the WBL model proposed by Hara and Belcher (2004), which is reviewed briefly here. The WBL is within a constant flux layer, and thus the total momentum flux τ^{tot} is constant with height. The downward total momentum flux τ^{tot} is composed of turbulent stress $\tau^t(z)$ and wave-induced stress $\tau^w(z)$, and thus the budget of the momentum flux is expressed as

$$\tau^{\text{tot}} = \rho_a u_*^2 = \tau^t(z) + \tau^w(z), \tag{6}$$

where u_* is the friction velocity of airflow. The origin of the z axis is the sea surface. The wave-induced stress is a momentum flux due to periodic motion in the airflow caused by wind waves. The wave-induced stress at the wave surface $\tau^w(0)$ governs the growth and decay of wind waves and is expressed as (Makin and Mastenbroek 1996)

$$\tau^w(0) = \int_0^\infty \int_{-\pi/2}^{\pi/2} \beta_g(k', \theta)\rho_w \sigma\psi(k', \theta)\cos\theta\, d\theta k' dk', \tag{7}$$

where $\psi(k, \theta)$ is the wavenumber spectrum; and k, σ, θ, $\beta_g(k, \theta)$, and ρ_w are the wavenumber, wave angular frequency, wave propagation direction relative to the mean wind direction, wave growth rate, and density of water, respectively.

The wave-induced stress tends to decay with height. Hara and Belcher (2004) employed a step function to represent this decay behavior:

$$I(k, z) = 1 \quad z \le z_i(k),$$
$$I(k, z) = 0 \quad z > z_i(k). \tag{8}$$

Here, $z_i(k)$ is the depth of the inner region in the airflow over waves of wavenumber k. Hara and Belcher (2004) set $kz_i(k) = \delta$, where δ is a constant of $O(0.05)$ used as a fitting parameter. Using this decay function, the wave-induced stress at a height z is given by

$$\tau^w(z) = \int_0^{\delta/z} \int_{-\pi/2}^{\pi/2} \beta_g(k', \theta)\rho_w \sigma \psi(k', \theta) \cos\theta \, d\theta k' \, dk'. \tag{9}$$

The local turbulent stress $\tau^t(z = \delta/k)$ at the top of the inner region for waves of wavenumber k is given by

$$\tau^t[z = z_i(k)] = \rho_a[u_*^l(z)]^2 = \tau^{\text{tot}} - \tau^w(z), \tag{10}$$

where $u_*^l[z = z_i(k)]$ is the local friction velocity. The local turbulent stress $\tau^t(z = \delta/k)$ forces waves of wavenumber k (Belcher and Hunt 1993); thus, the growth rate $\beta_g(k, \theta)$ for waves of wavenumber k is estimated using the local turbulent stress. Solving the momentum flux budget above affords the vertical distribution of the local turbulent stress.

To calculate the vertical distribution of the mean wind velocity, Hara and Belcher (2004) considered the total kinetic energy conservation in the WBL, that is, the sum of the kinetic energy of the mean motions, wave-induced motion, and turbulence, as expressed by

$$\frac{d}{dz}(u\tau^{\text{tot}}) + \frac{d\Pi}{dz} + \frac{d\Pi'}{dz} - \rho_a \varepsilon = 0, \tag{11}$$

where ε is the viscous dissipation of turbulent kinetic energy, and Π and Π' are the vertical transport of kinetic energy of wave-induced motion and the vertical transport of turbulent kinetic energy, respectively. It was assumed that the largest contribution to Π is from pressure transport, while the decay of Π is governed by the same decay function as the wave-induced stress:

$$\Pi(z) = \int_0^{\delta/z} \int_{-\pi}^{\pi} \beta_g(k', \theta)\rho_w g \psi(k', \theta) \, d\theta k' \, dk', \tag{12}$$

where g is the acceleration of gravity. It was further assumed that the divergence of turbulent transport within the WBL is smaller than the other terms in Eq. (11), because the WBL is a homogeneous rough-wall boundary layer, and can thus be neglected. The viscous dissipation $\varepsilon(z)$ is related to the local friction velocity $u_*^l(z)$ at each height and is approximated by $\varepsilon = u_*^l(z)^3/\kappa z$. Solving the kinetic energy budget allows the vertical distribution of the mean wind velocity to be estimated.

For fast-moving waves $[k > k_m = 0.07^2 g/(u_*^l)^2]$, the growth rate $\beta_g(k, \theta)$ is negligible. Thus, as Eq. (9) shows, the effect of wind waves does not extend above $z_m = \delta/k_m$, where the height z_m is defined as the top of the WBL, above which τ^t is constant. For detailed procedures for solving the WBL model, refer to Hara and Belcher (2004) or Moon et al. (2004a).

b. Scalar transfer in WBL

Scalar transfer in the WBL is evaluated following the approach of Makin and Mastenbroek (1996). In the WBL, the total scalar flux is constant with height, as expressed by

$$H_\Theta^{\text{tot}} = H_\Theta^t(z) + H_\Theta^w(z), \tag{13}$$

where H_Θ^t and H_Θ^w denote the turbulent scalar flux and the wave-induced scalar flux of a scalar Θ. It is assumed that the wave-induced scalar flux H_Θ^w is negligible, because it is much smaller than the turbulent scalar flux. This assumption is considered acceptable because the wave-induced scalar fluxes at the sea surface and the top of the WBL are zero and the depth of the WBL estimated by solving the WBL model of Hara and Belcher (2004) is thin, as shown by Moon et al. (2004a), who show that the depth is 1.4 m for the mature sea state under $u_{10} = 45$ m s^{-1} (cf. their Fig. 9).

Using the eddy viscosity assumption, the relationship between scalar flux and the vertical distribution of the concentration of Θ is determined by relating the local turbulent stress to the vertical gradient of the mean velocity:

$$\tau^t(z) = \rho_a K_m(z) \frac{du}{dz}, \tag{14}$$

where K_m is the eddy viscosity. Similarly, the turbulent scalar flux is expressed as

$$H_\Theta^t(z) = \frac{K_m(z)}{\text{Sc}_{\Theta t}} \frac{d\Theta}{dz}. \tag{15}$$

Here, $\text{Sc}_{\Theta t} = K_m/K_\Theta$ is the turbulent Schmidt number of Θ, where K_Θ is the eddy diffusivity of Θ. If Θ denotes the temperature T, then the turbulent Schmidt number denotes the turbulent Prandtl number $\text{Pr}_t = K_m/K_s$, where K_s is the eddy diffusivity of sensible heat, and the upward turbulent sensible heat flux $H_s{}^t$ is expressed as

$$H_S^t(z) = -\rho_a c_{\mathrm{pa}} \frac{K_m(z)}{\mathrm{Pr}_t} \frac{dT}{dz}. \quad (16)$$

In the case of turbulent latent heat flux H_L^t,

$$H_L^t(z) = -\rho_a L_E \frac{K_m(z)}{\mathrm{Sc}_t} \frac{dq}{dz}, \quad (17)$$

where Sc_t is the Schmidt number of water vapor. The boundary condition for q at the sea surface is q_w. As the exchange bulk coefficients for sensible heat flux and latent heat flux are almost identical in many sets of observational results, Sc_t for water vapor can be assumed to be approximately equal to Pr_t. The turbulent sensible and latent heat fluxes [$H_S^t(0)$, $H_L^t(0)$] represent interfacial heat transfer.

It should be noted that although the wave-induced scalar flux H_Θ^w in Eq. (13) is ignored, the effects of wind waves are indirectly reflected in the scalar transfer through the use of the local turbulent stress τ^t in Eq. (14), which is derived from the WBL model.

c. Sea spray–mediated heat transfer

The effect of sea spray on heat transfer is evaluated by applying the sea spray–mediated heat flux parameterization proposed by Fairall et al. (1994). This parameterization allows the effects of the evaporation of oceanic spray droplets on the sensible and latent heat fluxes to be determined using bulk meteorological quantities such as wind velocity, temperature, and relative humidity (RH) at a height of 10 m and at sea surface temperature.

Fairall et al.'s (1994) parameterization is based on the droplet microphysics model of Andreas (1990, 1992). In Andreas (1990), three time scales were introduced for droplets in relation to sea spray–mediated heat transfer; the time scales of temperature evolution (τ_T), evaporation (τ_r), and atmospheric resistance for a droplet (τ_f). The time scale of temperature evolution determines the time necessary for a droplet to reach its equilibrium temperature, while τ_r represents the time necessary for a droplet to reach its equilibrium radius and is two to three orders of magnitude longer than τ_T. Droplets thus exchange sensible heat much more rapidly than latent heat (Andreas 1992). The time scale of atmospheric resistance for a droplet determines the duration the droplet exchanges sensible and latent heat with the ambient atmosphere. These three time scales are dependent on the initial radius of droplets. Fairall et al. (1994) integrated the heat exchanges among initial radii r_0, satisfying the relation

$$\tau_T(r_0) \le \tau_f(r_0) \le \tau_r(r_0). \quad (18)$$

The sensible and latent heat exchange for droplets occurs within a DEL, the height of which can be approximated by the significant wave amplitude a_s (i.e., half the significant wave height h_s). According to Eq. (18), the droplets transfer all excess sensible heat to the ambient atmosphere in the DEL. The sea spray–mediated sensible heat flux in the DEL is parameterized as

$$Q_s = \rho_w c_{\mathrm{pw}} W(u_{10}) S_v (T_w - T_{z=a_s}), \quad (19)$$

where ρ_w and c_{pw} denote the density and specific heat of water. Here, $W(u_{10})$ is the whitecap area fraction, which is related to the sea spray–generation function dF/dr_0 as

$$\frac{dF}{dr_0} = W(u_{10}) f(r_0). \quad (20)$$

Here, $f(r_0)$ is the source spectrum per unit area of whitecap. As the sea spray–generation function proposed by Andreas (1992) applies to an upper limit of wind velocity of 20 m s^{-1}, application of the parameterization of Fairall et al. (1994) to strong wind conditions such as those for tropical cyclones requires a new generation function corresponding to stronger winds. Here, the generation function proposed by Andreas (1998) is employed, which can be applied to wind conditions of up to 32 m s^{-1}. Corresponding to the new generation function, new values of $W(u_{10})$ and S_v in Eq. (19) are used because $S_v = \int_0^\infty (4\pi/3) r^3 f(r)\, dr$. After some arithmetic, we obtain

$$W(u_{10}) S_v = \alpha_1 g_1(u_{14}) + \alpha_2 g_2(u_{14}). \quad (21)$$

Here,

$$\alpha_1 = 5.52 \times 10^{-14}\ \mathrm{m\ s^{-1}},$$

$$\alpha_2 = 1.03 \times 10^{-10}\ \mathrm{m\ s^{-1}},$$

$$\log[g_1(u_{14})] = 0.0676 u_{14} + 3.43, \quad (22)$$

and

$$\log[g_2(u_{14})] = 0.959 u_{14}^{1/2} - 0.476, \quad (23)$$

where u_{14} is the wind velocity at a height of 14 m, which can be estimated by solving the present model.

The evaporation of droplets is assumed in Fairall et al. (1994) to occur constantly in the DEL. The sea spray–mediated latent heat flux is thus parameterized as

$$Q_L = \rho_a L_E W(u_{10}) S_a a_s \beta(T_{z=a_s})[q_s(T_{z=a_s}) - q_{z=a_s}], \quad (24)$$

where $q_s(T_{z=a_s})$ is the saturation-specific humidity for the temperature at the height a_s, and β is given by

$$\beta = \left[1 + \frac{0.622L_E^2}{R_d c_{\mathrm{pa}} T_{z=a_s}{}^2} q_s(T_{z=a_s})\right]^{-1}, \tag{25}$$

where R_d is the gas constant for dry air. As the new generation function of Andreas (1998) is used here, the value of $W(u_{10})S_a$ must be estimated. Using the value estimated based on the definition of Fairall et al. (1994) to evaluate the latent heat flux mediated by sea spray under the same meteorological conditions as considered in Andreas (1992) over mature seas, the latent heat fluxes given by the present model are one order of magnitude smaller than those reported by Andreas (1992). The value of $W(u_{10})S_a$ is thus modified by multiplying by a constant, as given by

$$W(u_{10})S_a = \gamma_1 g_1(u_{14}) + \gamma_2 g_2(u_{14}), \tag{26}$$

where $\gamma_1 = 1.10 \times 10^{-9}$ and $\gamma_2 = 2.05 \times 10^{-6}$.

As the sensible and latent heat fluxes are constant in the constant flux layer, the total sensible and latent heat fluxes are expressed as

$$H_S^{\mathrm{tot}} = H_S^t(z) + H_S^w(z) + Q_S(z) - Q_L(z), \tag{27}$$

$$H_L^{\mathrm{tot}} = H_L^t(z) + H_L^w(z) + Q_L(z). \tag{28}$$

Here, the sea spray–mediated heat fluxes are assumed to be constant values estimated from Eqs. (19) and (24) in the DEL and to vanish above the DEL. This assumption means that sea spray droplets are generated at the top of the DEL and the heat exchange between the sea spray droplets and the ambient atmosphere occurs only at the top of the DEL. Although heat exchange will actually occur everywhere in the DEL, information on the heat exchange in the DEL is not sufficient to be able to determine the vertical profiles of $Q_S(z)$ and $Q_L(z)$. Thus, the validity of this assumption remains to be verified in future work.

The upward turbulent sensible and latent heat fluxes at a reference height higher than the DEL is expressed as

$$\underbrace{H_S^t(z)}_{z>a_s} = \underbrace{H_S^t(z) + H_S^w(z) + Q_S - Q_L}_{z\le a_x}, \tag{29}$$

$$\underbrace{H_L^t(z)}_{z>a_s} = \underbrace{H_L^t(z) + H_L^w(z) + Q_L}_{z\le a_x}. \tag{30}$$

Because the WBL is much thinner than the DEL, the turbulent sensible and latent heat fluxes are constant above the DEL. Furthermore, because the wave-induced scalar flux is assumed to be negligible, the turbulent heat fluxes are also constant below the DEL. Thus, Eqs. (29) and (30) can be rewritten as

$$H_{Sz>a_s}^t = H_{Sz\le a_s}^t + Q_S - Q_L, \tag{31}$$

$$H_{Lz>a_s}^t = H_{Lz\le a_s}^t + Q_L. \tag{32}$$

Here, $H_{Sz\le a_s}^t$ and $H_{Lz\le a_s}^t$ denote the interfacial sensible and latent heat fluxes, and $H_{Sz>a_s}^t$ and $H_{Lz>a_s}^t$ denote the total sensible and latent heat fluxes.

d. Effects of stable/unstable stratification

Using the bulk meteorological quantities at a height of 10 m and at sea surface (i.e., u_{10}, T_{10}, q_{10}, T_w, q_w), the fluxes are estimated by solving the WBL model and sea spray model. The profiles of the vertical gradients of wind velocity, temperature, and specific humidity [i.e., $du/dz = f_u(z)$, $dT/dz = f_T(z)$, and $dq/dz = f_q(z)$] are also obtained. Note that the obtained values of $f_u(z)$, $f_T(z)$, and $f_q(z)$ are under a neutral condition. As bulk meteorological quantities contain stratification effects, the buoyancy effects on turbulent transfer should be taken into account. Following the Monin–Obukhov similarity, the vertical gradients are corrected in the cases of stably/unstably stratified airflow as

$$du/dz = f_u(z)\phi_u(z/L), \tag{33}$$

$$dT/dz = f_T(z)\phi_T(z/L), \tag{34}$$

$$dq/dz = f_q(z)\phi_q(z/L), \tag{35}$$

where L is the Monin–Obukhov length defined by

$$L^{-1} = -\left(\frac{g\kappa}{u_*^3 T_w}\right)\left[\frac{H_S^t(z)}{\rho_a c_{\mathrm{pa}}} + \frac{0.61T_w}{1+0.61q_w}\frac{H_L^t(z)}{\rho_a L_E}\right]. \tag{36}$$

Note that the turbulent sensible and latent heat fluxes (i.e., H_S^t and H_L^t) are distributed like a step function: they are constant below and above $z = a_s$, but vary rapidly at $z = a_s$. Thus, the value of L below $z = a_s$ is different from that above $z = a_s$.

The stratification corrections for the unstable condition (i.e., $L < 0$) are given by (Kondo 1994):

$$\phi_u(z/L) = [1 - 16(z/L)]^{-1/4} \tag{37}$$

and

$$\phi_T(z/L) = \phi_q(z/L) = [1 - 16(z/L)]^{-1/2}. \tag{38}$$

The stratification corrections for the stable condition (i.e., $L > 0$) are given by

$$\phi_u(z/L) = \phi_T(z/L) = \phi_q(z/L) = 1 + 7(z/L). \tag{39}$$

In the present study, these stratification effects are accounted for by performing iterative calculations. First, the WBL model and sea spray model are solved under a neutral condition (i.e., $\phi_u = \phi_T = \phi_q = 1$), and we obtain the turbulent momentum, sensible and latent heat fluxes, and the value of $f_u(z)$, $f_T(z)$, and $f_q(z)$. Then, L and the stratification corrections (i.e., ϕ_u, ϕ_T, and ϕ_q) are calculated by using the turbulent fluxes. We substitute the values of L and the stratification corrections into Eqs. (33)–(35), and we solve the WBL model and sea spray model again. The iteration continues until the fluxes reach appropriate convergence limits.

e. Solving procedure

Using bulk meteorological quantities and the wavenumber spectrum $\psi(k, \theta)$ for a mature wave state, the sensible and latent heat transfer under the effects of surface waves and sea spray is calculated. The bulk meteorological quantities include the wind velocity, temperature, and relative humidity at a height of 10 m and at the temperature and atmospheric pressure at the sea surface.

A wavenumber spectrum near the peak frequency proposed by Elfouhaily et al. (1997) is adopted here. This wavenumber spectrum is based on the wavenumber spectra proposed by Pierson and Moskowitz (1964) and the Joint North Sea Wave Project (JONSWAP) (Hasselmann et al. 1973) for a low-wavenumber regime, and the wavenumber spectra of Phillips (1985) and Kitaigorodskii (1973) for a high-wavenumber regime. The wavenumber spectrum $\psi(k, \theta)$ of Elfouhaily et al. have a relatively simple closed form and are consistent with past observational results. Further, $\psi(k, \theta)$ can be considered to represent a saturation value based on the wave age (c_P/u_{10}) or fetch, where c_P is the wave velocity of the peak frequency. In the present study, the mature sea state is considered, for which c_P/u_{10} is set at 1.19 (Elfouhaily et al. 1997).

In the high-wavenumber regime, which is considered to be an equilibrium range (Phillips 1977), the wavenumber spectrum of Hara and Belcher (2002) is employed. An equilibrium wave state is maintained by the balance of energy among the three sources of wave action: input from wind, dissipation due to wave breaking, and divergence of wave action flux by nonlinear wave interactions (Phillips 1985). The analytical model for $\psi(k, \theta)$ presented by Hara and Belcher (2002) is developed by introducing energy input sources obtained from the WBL model of Hara and Belcher (2004). Thus, $\psi(k, \theta)$ in the equilibrium range of Hara and Belcher (2002) is regarded as appropriate for solving the WBL model of Hara and Belcher (2004).

Hara and Belcher (2002) identify a sheltering wavenumber (k_s) at which the local turbulent stress begins to be affected by sheltering by longer waves. The wavenumber spectrum in the equilibrium range $[\psi_{eq}(k, \theta)]$ is thus expressed as

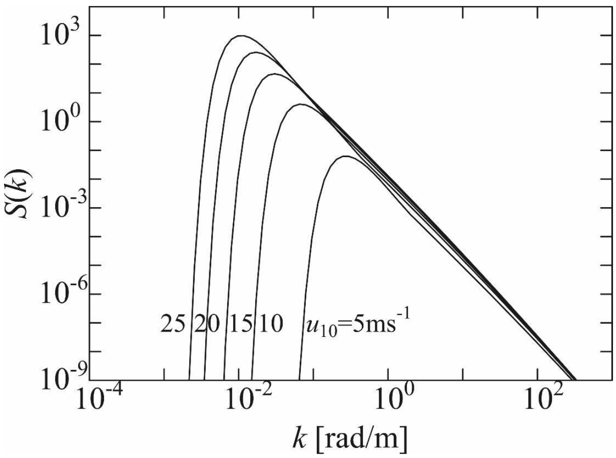

FIG. 1. Distributions of the omnidirectional spectrum $S(k)$ for a mature sea for u_{10} = 5, 10, 15, 20, and 25 m s^{-1}.

$$\psi_{eq}(k, \theta) = \frac{1}{40c_\theta}\left[1 + \left(\frac{k_s}{k}\right)^{1/2}\right]^{-1} h(\theta)^{1/2}k^{-4}. \tag{40}$$

Here, $h(\theta) = \cos^2(\theta)$ for $-\pi/2 < \theta < \pi/2$, $h(\theta) = 0$ for $|\theta| \geq \pi/2$, and $c_\theta = \int_{-\pi}^{\pi} [h(\theta)]^{3/2} \cos\theta d\theta = 3\pi/8$. The sheltering wavenumber is determined by continuously joining the omnidirectional spectrum $S(k) = \int_{-\pi}^{\pi} \psi(k, \theta)\, k d\theta$ of the equilibrium range with that of the lower wavenumber at the cutoff wavenumber (k_c). Following Moon et al. (2004a), k_c is set at $9.0 \times k_{\text{peak}}$, where k_{peak} is the wavenumber of the peak frequency. The sheltering wavenumber is then given by

$$k_s = k_c\left[\frac{k_c^{-4}}{40c_\theta}\frac{\displaystyle\int_{-\pi}^{\pi} h(\theta)^{1/2}\, d\theta}{\displaystyle\int_{-\pi}^{\pi} \psi(k_c, \theta)\, d\theta} - 1\right]^2. \tag{41}$$

Figure 1 shows the distribution of the omnidirectional spectrum $S(k)$ for a mature sea at several wind velocities. This omnidirectional spectrum includes the peak frequency regime of Elfouhaily et al. (1997) and the equilibrium regime of Hara and Belcher (2002). The figure shows that these two regimes are smoothly connected.

The WBL model of Hara and Belcher (2004) is then solved following Moon et al. (2004a). The upper bound of wavenumber (k_1) is set at 400 rad m^{-1}, above which Hara and Belcher (2004) showed that the calculated roughness length of momentum does not depend on the value of k_1. The boundary condition at the sea surface

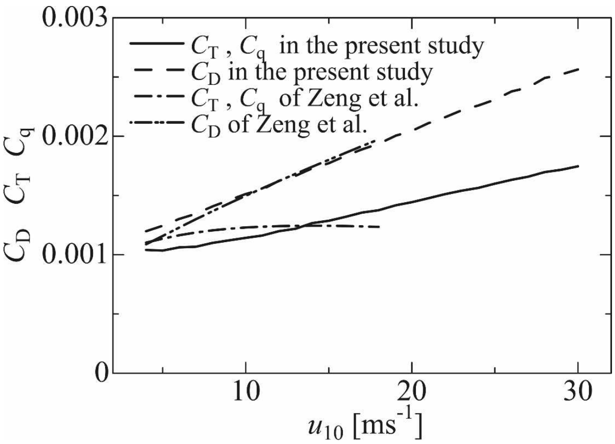

FIG. 2. Wind speed dependence of exchange coefficients C_D, C_T, and C_q for mature sea states obtained in the present study. Those reported by Zeng et al. (1998) are also shown. The solid line denotes C_T and C_q in the present study; the dashed line is C_D in the present study; the chain line is C_T and C_q of Zeng et al.; and the chain double-dashed line is C_D of Zeng et al.

is defined by $u(z = \delta/k_1) = 0$ at $z = 0.1v_a/u^l_*(k_1)$. The value of δ is set at 0.008, such that the drag coefficient for the mature sea state is consistent with the parameterization of Zeng et al. (1998) for weak to moderate winds ($4 \le u_{10} \le 18$ ms^{-1}), as shown in Fig. 2. Solving the WBL model, we can obtain the total momentum flux τ^{tot}, or friction velocity u_*, and the vertical distributions of local turbulent stress $\tau^t(z)$ and wind velocity $u(z)$.

Next, using the vertical distributions of $\tau^t(z)$ and $u(z)$, the relationship between the turbulent heat fluxes (constant in the WBL) and the vertical distributions of temperature or specific humidity is obtained from Eqs. (14), (16), and (17). Thus, the relationship between the turbulent heat fluxes and the temperature/specific humidity at the top of the WBL ($z = z_m$) can be expressed as

$$T_{z=z_m} = T_w - \frac{\mathrm{Pr}_t \sigma_{z=z_m} H^t_S}{\rho_a c_{\mathrm{pa}}} \tag{42}$$

and

$$q_{z=z_m} = q_w - \frac{\mathrm{Sc}_t \sigma_{z=z_m} H^t_L}{\rho_a L_E}, \tag{43}$$

where $\sigma_{z=z_m} = \int_{z_{0T}}^{z_m} K_m(z)^{-1}\,dz$ is a value obtained by solving the WBL model. For the boundary condition at the sea surface, $T(z_{0T}) = T_{\mathrm{w}}$ is set at $z_{0T} = 0.18v_a/u^l_*(k_1)$ (Liu et al. 1979), and $q(z_{0q}) = q_{\mathrm{w}}$ is set at $z_{0q} = z_{0T}$. The values of Pr_t and Sc_t are set at 1.1, such that the exchange coefficients of sensible and latent heat fluxes without sea spray effects agree with the parameterization of Zeng et al. (1998; see Fig. 2).

The sea spray–mediated heat fluxes are then determined by solving Eqs. (19), (24),

$$T_{z=a_s} = T_w - \frac{\mathrm{Pr}_t}{\rho_a c_{\mathrm{pa}}}\left[\sigma_{z=z_m} + \frac{1}{\kappa u_*}\ln\left(\frac{a_s}{z_m}\right)\right]H^t_{Sz\le a_s}, \tag{44}$$

$$q_{z=a_s} = q_w - \frac{\mathrm{Sc}_t}{\rho_a L_E}\left[\sigma_{z=z_m} + \frac{1}{\kappa u_*}\ln\left(\frac{a_s}{z_m}\right)\right]H^t_{Lz\le a_s}, \tag{45}$$

$$T_{10} = T_{z=a_s} - \frac{1}{\rho_a c_{\mathrm{pa}}}\frac{\mathrm{Pr}_t}{\kappa u_*}\ln\left(\frac{10}{a_s}\right)(H^t_{Sz\le a_s} + Q_S - Q_L), \tag{46}$$

and

$$q_{10} = q_{z=a_s} - \frac{1}{\rho_a L_E}\frac{\mathrm{Sc}_t}{\kappa u_*}\ln\left(\frac{10}{a_s}\right)(H^t_{Lz\le a_s} + Q_L). \tag{47}$$

Equations (44)–(47) are derived from Eqs. (16), (17), (31), and (32). As these six equations contain six unknown quantities (i.e., $T_{z=a_s}$, $q_{z=a_s}$, $H^t_{Sz\le a_s}$, $H^t_{Lz\le a_s}$, Q_S, Q_L), the equations can be solved. The effects of stratification are accounted for by solving these equations iteratively.

3. Results and discussion

a. Heat transfer over a mature sea without sea spray

The sensible and latent heat fluxes affected by fully developed ocean waves without sea spray effects (i.e., for the case that heat is transferred only from the ocean interface) are compared here with the results of the bulk algorithm of Zeng et al. (1998). Their algorithm is based on data obtained by TOGA COARE under weak to moderate wind conditions (<12 m s^{-1}) (Fairall et al. 1996), and in the HEXOS experiment under stronger wind conditions (<18 m s^{-1}) (DeCosmo et al. 1996). The roughness length of momentum (z_0), temperature (z_T), and humidity (z_q) are given by

$$z_0 = 0.013\frac{u_*^2}{g} + 0.11\frac{v_a}{u_*} \tag{48}$$

and

TABLE 1. Comparison of sea spray–mediated sensible and latent heat fluxes obtained in the present study (fourth and fifth columns) with those of Andreas (1992) (sixth and seventh columns). For every case, the wind velocity is 20 m s^{-1}.

T_{10} (°C)	T_w (°C)	RH	Q_S (W m^{-2}) (present study)	Q_L (W m^{-2}) (present study)	Q_S (W m^{-2}) (Andreas)	Q_L (W m^{-2}) (Andreas)
−10	0	80	32.3	46.5	33	61
−10	0	90	32.2	23.6	32	28
−0.1	0	80	0.9	79.2	3.8	87
5	0	80	−14.7	92.6	−12	100
20	17	80	−8.1	151.5	−2.5	150
27	29	80	7.5	183.2	16	170

$$z_T = z_q = z_0 \exp(-2.67\,\mathrm{Re}_*^{1/4} + 2.57), \tag{49}$$

where $\mathrm{Re}_* = u_* z_0/\upsilon_a$ is the roughness Reynolds number. Figure 2 shows the exchange coefficients (C_D, C_T, C_q) for mature sea states obtained in the present study along with those reported by Zeng et al. (1998). Here, the coefficients are defined as

$$C_D = \left(\frac{u_*}{u_{10}}\right)^2, \tag{50}$$

$$C_T = \frac{H_S^{\mathrm{tot}}}{\rho_a c_{\mathrm{pa}} u_{10}(T_w - T_{10})}, \tag{51}$$

and

$$C_q = \frac{H_L^{\mathrm{tot}}}{\rho_a L_E u_{10}(q_w - q_{10})}. \tag{52}$$

For this calculation, $T_w = 300$ K, $T_{10} = 298$ K, RH is set at 80%, and the atmospheric pressure (P_0) is 1000 hPa. The values of δ and Pr_t are set such that the coefficients match those of Zeng et al. (1998), as described in the previous section. The exchange coefficient of latent heat flux coincides with that of sensible heat flux if sea spray effects are not incorporated, because Pr_t is assumed to agree with Sc_t in Eqs. (16) and (17). Figure 2 shows that although the dependence of C_D on wind velocity is consistent among the results shown, slight differences can be observed among the results for C_T. Such differences can be attributed to the wide scattering of heat flux data in TOGA COARE and HEXOS observations (see Fairall et al. 1996; DeCosmo et al. 1996). The C_T and C_q parameterized from the HEXOS data of DeCosmo et al. (1996) exhibit ranges of approximately 60%, and the present results fall well within this scattering range of data. Thus, C_T and C_D obtained in the present study are considered acceptable for weak to moderate winds ($4 \le u_{10} \le 18$ m s^{-1}).

b. Heat transfer over a mature sea with sea spray

To evaluate the sensible and latent heat fluxes over mature sea states considering the effects of sea spray, the depth of the DEL (a_s) is required. Here, a_s is estimated using $\psi(k, \theta)$ by (Komen et al. 1994)

$$a_s = \frac{1}{2} h_s = 2 \times \int_0^\infty \int_{-\pi}^{\pi} \psi(k', \theta)\, d\theta k'\, dk'. \tag{53}$$

In Table 1, the present results are compared with those determined using the microphysics of Andreas (1992). The table lists the sea spray–mediated sensible and latent heat fluxes under the six conditions tabulated in Table 3 of Andreas (1992). The wind speed is fixed at $u_{10} = 20$ m s^{-1}, while the temperatures (T_{10}, T_w) and RH vary among cases. As can be seen in the table, the present results are generally in agreement with those of Andreas (1992), although the sensible heat flux at the lowest low in Table 1 is underestimated in the present model. This may indicate that the value of $W(u_{10})S_v$ in Eq. (19) need to be better regulated to agree with the results of Andreas (1992).

At the condition of the lowest low in Table 1, the interfacial turbulent sensible heat flux was 63.3 W m^{-2}, which is much smaller than Q_L (=183.2 W m^{-2}), and thus the total sensible heat flux is downward, even though T_{10} is lower than T_w. Similarly, in Andreas (1992), the corresponding interfacial turbulent sensible heat flux is 46 W m^{-2} using a bulk algorithm (Large and Pond 1981; Andreas and Murphy 1986), and it is also much smaller than Q_L (=170 W m^{-2}). In this case, the sea spray from the warmer ocean makes the cool atmosphere cooler, and this cooling and moistening effect would influence the tropical cyclone intensity (e.g., Kepert et al. 1999; Lighthill et al. 1994).

Figure 3 shows the effects of sea spray and surface waves on the vertical profiles of temperature and specific humidity under moderate ($u_{10} = 7$ m s^{-1}) and strong ($u_{10} = 25$ m s^{-1}) winds for a stably stratified condition with $T_w = 300$ K, $T_{10} = 302$ K, $P_0 = 1000$ hPa, and RH set at 80%. The calculated heat fluxes for the moderate wind case are $Q_S = -0.08$ W m^{-2}, $Q_L = 0.35$ W m^{-2}, $H_S^{\mathrm{tot}} = -12.28$ W m^{-2}, and $H_L^{\mathrm{tot}} = 27.55$ W m^{-2}, while those for the strong wind case are $Q_S = -14.4$ W m^{-2}, $Q_L = 855.4$ W m^{-2}, $H_S^{\mathrm{tot}} = -921.2$ W m^{-2},

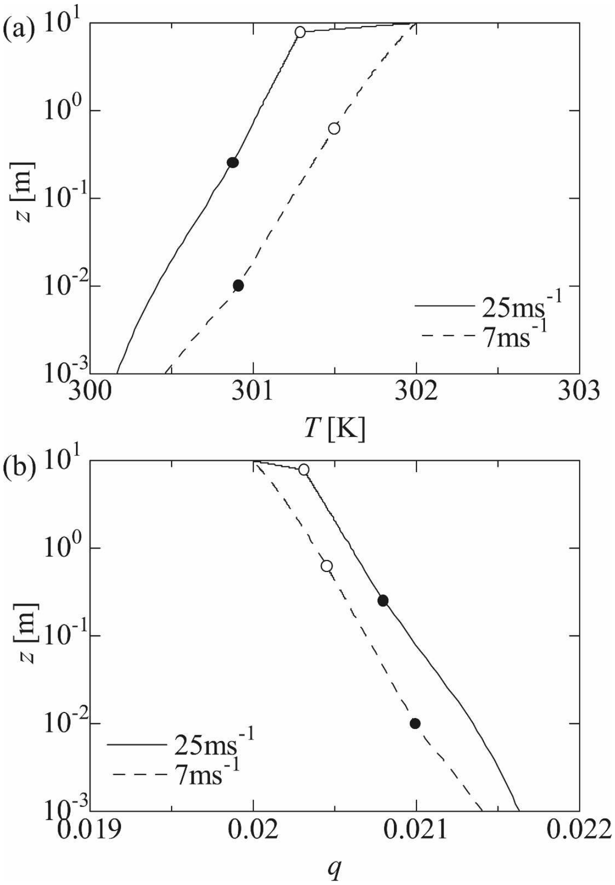

FIG. 3. (a) Vertical profiles of temperature and (b) specific humidity for u_{10} = 7 and 25 m s^{-1} under a stably stratified condition, with T_w = 300 K, t_{10} = 30 2K, RH = 80%, and P_0 = 1000 hPa. A black circle denotes the height of the top of the wave boundary layer; an open circle denotes the height of the top of the drop evaporation layer.

and H_L^{tot} = 1006.8 W m^{-2}. For the moderate wind conditions, the magnitudes of sea spray–mediated heat fluxes are much smaller than those of the total heat fluxes, and the sea spray would have little effect on the heat transfer mechanism. Under strong wind conditions, on the other hand, the sea spray–mediated latent heat flux is comparable in magnitude to the total heat fluxes; thus, the sea spray effect would be strong.

Figure 3 shows that the WBL is much thinner than the DEL, but becomes thicker with increasing wind speed. Although the temperature and specific humidity are approximately distributed logarithmically above the WBL, the distributions in the WBL are not logarithmic. The vertical gradient of temperature just below the top of the WBL (at approximately z = 0.1 m at 25 m s^{-1}) is larger than that extrapolated from the logarithmic layer (at approximately z = 1 m at 25 m s^{-1}), attributable to the wave-induced kinetic energy in Eq. (11), which decreases with height [i.e., $d\Pi/dz$ in Eq. (11) is negative]. Thus, the vertical gradient of velocity and eddy viscosity in the WBL become larger than those above the WBL, resulting in a corresponding increase in the modulus of the vertical gradient of temperature and humidity. If the vertical transport of kinetic energy of the wave-induced motion is not considered in Eq. (11), the vertical gradient of temperature just below the WBL becomes smaller than that in the logarithmic layer, because the modulus of the vertical gradient of temperature in this case is expressed as

$$\left|\frac{dT}{dz}\right| = \frac{\mathrm{Pr}_t}{\rho_a c_{\mathrm{pa}}}\frac{1}{\kappa z u_*}\left(\frac{{u_*}^l(z)}{u_*}\right)|H^t_{Sz\le z_m}|$$
$$\le \frac{\mathrm{Pr}_t}{\rho_a c_{\mathrm{pa}}}\frac{1}{\kappa z u_*}|H^t_{Sz\le z_m}|. \qquad (54)$$

For moderate winds, the contributions of sea spray–mediated fluxes are much smaller than those of turbulent fluxes at the interface, and thus almost no changes are observed in the vertical gradients of T and q at the top of the DEL (i.e., at $z = a_s$). However, because of the effect of stable stratification, the vertical gradients are misaligned with a logarithmic low near $z \cong 10$ m. For strong winds, on the other hand, the vertical gradient of T and q changes quickly at $z = a_s$. Strong winds generate substantial volumes of sea spray, and the evaporation of droplets cool the atmosphere in the DEL. The temperature below the DEL thus becomes lower than that without sea spray effects.

Figure 4 shows the vertical profiles of temperature and specific humidity for an unstably stratified condition with T_w = 300 K, T_{10} = 298 K, P_0 = 1000 hPa, and RH set at 80%. The values obtained for moderate wind are Q_S = 0.09 W m^{-2}, Q_L = 0.35 W m^{-2}, H_S^{tot} = 14.83 W m^{-2}, and H_L^{tot} = 113.81 W m^{-2}, and those for strong wind are Q_S = 27.5 W m^{-2}, Q_L = 821.7 W m^{-2}, H_S^{tot} = −693.8 W m^{-2}, and H_L^{tot} = 1398.6 W m^{-2}. As is the case with the stably stratified condition, the magnitudes of sea spray–mediated heat fluxes are much smaller than those of the total heat fluxes under moderate wind conditions, whereas the magnitude of sea spray–mediated latent heat flux is comparable to that of the total heat fluxes under strong wind conditions. Thus, under moderate wind conditions, the contributions of sea spray–mediated fluxes are much smaller than those of turbulent fluxes at the interface, and almost no changes are observed in the vertical gradients of T and q at the top of the DEL. For strong wind, the sign of the vertical gradient of T changes at $z = a_s$, because the turbulent sensible heat flux above the DEL

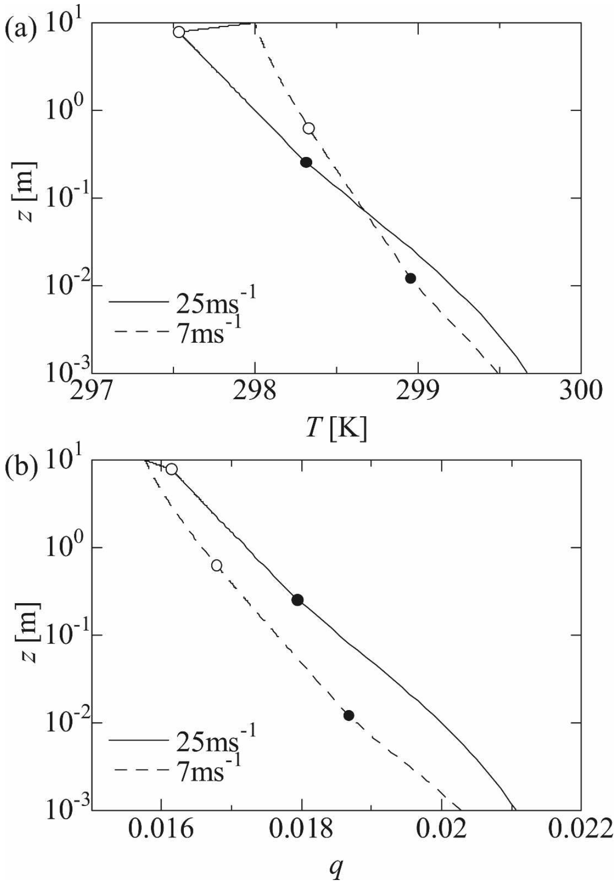

FIG. 4. (a) Vertical profiles of temperature and (b) specific humidity for u_{10} = 7 and 25 m s^{-1} under an unstably stratified condition, with T_w = 300 K, T_{10} = 298 K, RH = 80%, and P_0 = 1000 hPa. A black dot denotes the height of the top of the wave boundary layer; an open circle denotes the height of the top of the drop evaporation layer.

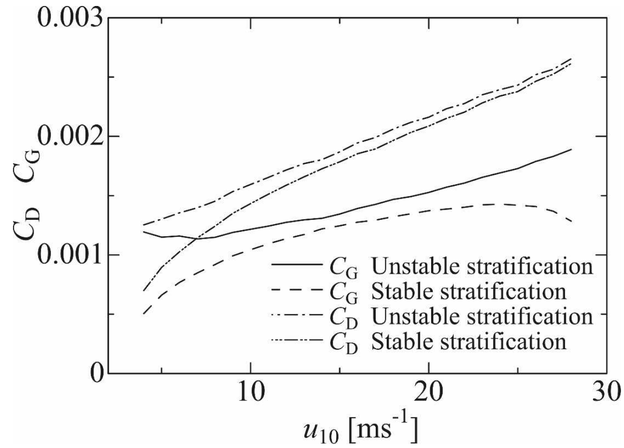

FIG. 5. Wind speed dependence of the exchange coefficient of total enthalpy C_G and the drag coefficient C_D under stably and unstably stratified conditions. The solid line denotes C_G under the unstably stratified condition; the dashed line is C_G under the stably stratified condition; the chain line is C_D under the unstably stratified condition; and the chain double-dashed line is C_D under the stably stratified condition.

is negative while that below the DEL is positive. In this case, the temperature at $z = a_s$ is lower than T_{10}, resulting in larger sea spray–mediated sensible and latent heat fluxes than that estimated by Fairall's original parameterization, in which the temperature and specific humidity at $z = a_s$ in Eqs. (19) and (24) are approximated from T_{10} by

$$(T_w - T_{z=a_s}) = \left(1 - 0.087 \ln \frac{10}{a_s}\right)(T_w - T_{10}) \quad (55)$$

and

$$[q_s(T_{z=a_s}) - q_{z=a_s}] = \left(1 - 0.087 \ln \frac{10}{a_s}\right)[q_s(T_{10}) - q_{10}]. \quad (56)$$

The value of $(T_w - T_{z=a_s})$ in Eq. (19) is 1.96 K in Fairall's original parameterization for u_{10} = 25 m s^{-1}, while the value given by the present model is 2.46 K, resulting in larger Q_S and Q_L. Andreas and DeCosmo (2002) incorporated this cooling effect by reducing the feedback of Q_L to H_s^{tot}, effectively adjusting the heat fluxes by tuning the respective contributions.

The cooling effect also increases the interfacial sensible heat fluxes (i.e., $H^t_{Sz<a_s}$), because the turbulent sensible heat flux depends on the vertical gradient of temperature. This is an indirect contribution of sea spray evaporation to the total heat fluxes and would facilitate the development of tropical cyclones.

It should be noted that under such unstably stratified and strong wind conditions, the total enthalpy flux is upward but the total sensible heat flux is downward. The total enthalpy flux H_G is given by

$$H_G = H_S^{\mathrm{tot}} + H_L^{\mathrm{tot}} = [H^t_S + H^t_L]_{z\le a_s} + Q_S. \quad (57)$$

Emanuel (1995a) argued that the development of tropical cyclones is dependent on the total enthalpy flux. The exchange coefficients of total enthalpy (C_G) under stably and unstably stratified conditions are plotted in Fig. 5 for the wind speed range of $4 \le u_{10} \le 28$ m s^{-1}. Although the spray-generation function adopted here is applicable at wind speeds of up to u_{10} = 32 m s^{-1}, the top of the DEL under stronger winds ($u_{10} > 28$ m s^{-1}) exceeds 10 m (not shown). Under the stably stratified condition, T_w = 300 K, T_{10} = 302 K, P_0 = 1000 hPa, and RH is set at 80%. Under the unstably stratified condition, T_w = 300 K, T_{10} = 298 K, P_0 = 1000 hPa, and RH is set at 80%.

TABLE 2. The interfacial and sea spray–mediated heat fluxes under both stably and unstably stratified cases for the strongest wind condition (u_{10} = 28 m s^{-1}). The interfacial heat fluxes without sea spray effects are also shown. Under the stably stratified condition, we set T_w = 300 K, T_{10} = 302 K, RH = 80%, and P_0 = 1000 hPa. On the other hand, under the unstably stratified condition, we set T_w = 300 K, T_{10} = 298 K, RH = 80%, and P_0 = 1000 hPa.

	u_{10}	H_S^t (W m^{-2})	H_L^t (W m^{-2})	Q_S (W m^{-2})	Q_L (W m^{-2})
Unstably stratified, without sea spray	28	95	726	. . .	. . .
Unstably stratified, with sea spray	28	113	752	49	2256
Stably stratified, without sea spray	28	−94	217	. . .	. . .
Stably stratified, with sea spray	28	−81	211	−36	2356

For weak to moderate winds (4 ≤ u_{10} ≤ 12 m s^{-1}), the buoyancy effect on turbulence causes a difference in C_G among the two cases. In the stably stratified airflow, the turbulence becomes weak, causing C_G to become smaller than that in the neutral case, while under unstably stratified conditions, turbulence increases, resulting in higher C_G. In the case of strong winds (u_{10} > 20 m s^{-1}), the sea spray–mediated heat fluxes are responsible for the difference between the two cases. Table 2 lists the interfacial and sea spray–mediated heat fluxes for both cases under the strongest wind condition (u_{10} = 28 m s^{-1}), as well as the interfacial heat fluxes without sea spray effects. Under the stably stratified condition, the total enthalpy flux becomes positive, even though the interfacial and sea spray–mediated sensible heat fluxes are negative. Although the sea spray indirectly increases the interfacial heat fluxes by 7 W m^{-2} because of cooling in the DEL, the sea spray–mediated heat flux directly reduces the total enthalpy flux by 36 W m^{-2}, resulting in an overall decrease in total enthalpy flux. Under the unstably stratified condition, on the other hand, the large sea spray–mediated latent heat flux cools the DEL, and the interfacial heat fluxes are indirectly increased by 44 W m^{-2}. In conjunction with the direct increase in heat flux of 49 W m^{-2}, the combined effects increase the total enthalpy flux by approximately 10%. The numerical results of Wang et al. (2001) indicate that the parameterization of Fairall et al. (1994) results in a smaller direct contribution of sea spray to the total enthalpy flux than its indirect contribution in the tropical cyclone model. This is considered to be caused by the omission of the cooling effect below the reference height of bulk variables (i.e., z = 10 m), resulting in an underestimation of sea spray–mediated heat flux. Thus, the present model would give a larger total contribution by sea spray evaporation in the tropical cyclone model.

In the unstably stratified case, the increasing rate of C_G with wind speed under strong wind (u_{10} ≥ 20 m s^{-1}) is consistent with that for C_D. In other words, the dependence of C_G on wind speed is comparable to that for C_D under strong wind conditions. Figure 6 shows the ratio of C_G to C_D under the unstably stratified condition. The parameterization of Zeng et al. (1998) for a weak to moderate wind regime (4 ≤ u_{10} ≤ 18 m s^{-1}) and the extrapolation to a strong wind regime (18 ≤ u_{10} ≤ 28 m s^{-1}) are also plotted. While C_G/C_D given by the parameterization of Zeng et al. decreases with increasing wind speed, C_G/C_D in the present study reaches a plateau at 0.7 for strong winds (u_{10} ≥ 20 m s^{-1}). This result supports the theory of Emanuel (1995a); that is, the ratio C_G/C_D should be greater than 0.75 to maintain the intensity of a tropical cyclone.

The slightly lower value C_G/C_D = 0.7 (<0.75) in the present study may be due to an underestimation of the sea spray–mediated sensible heat flux Q_S. The lowest low of Table 1, which is a similar condition to Fig. 6, shows that the sea spray–mediated sensible heat flux Q_S in the present study is approximately half that reported by Andreas (1992). If the value of $W(u_{10})S_v$ in Eq. (19) is multiplied by a constant value of 2.2 to agree with our Q_S of the lowest low of Table 1 with that of Andreas (1992), the ratio increases with wind speed, reaching 0.75 at u_{10} = 27 m s^{-1} (see Fig. 6). Note that although

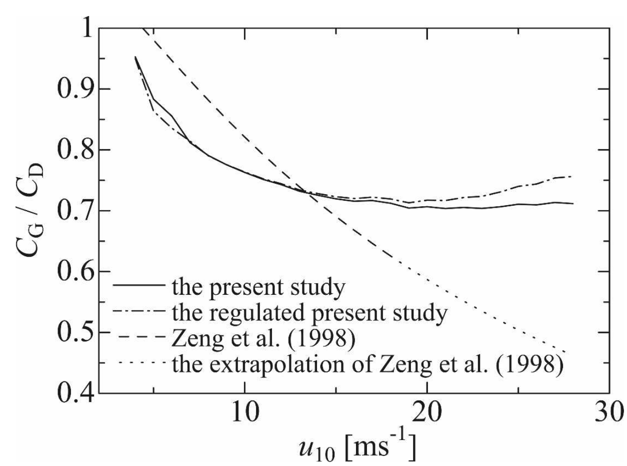

FIG. 6. Wind velocity dependence of C_G/C_D under an unstably stratified condition. The solid line denotes our result; the dashed line is the parameterization of Zeng et al. (1998); the dotted line is the extrapolation of the parameterization of Zeng et al.; and the chain line is our regulated result.

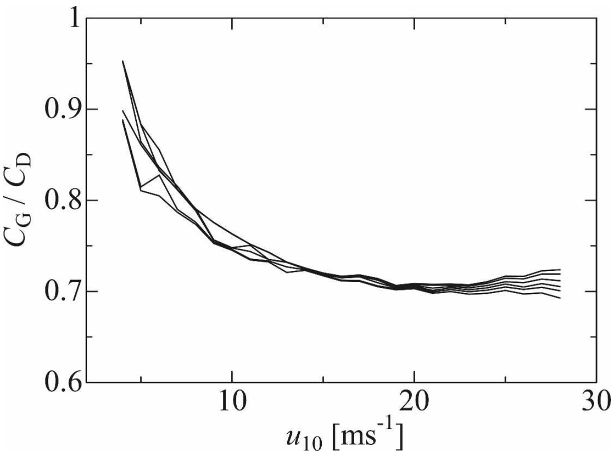

FIG. 7. Wind velocity dependence of C_G/C_D under unstably stratified conditions. The temperature difference $T_w - T_{10}$ varies from 0.5 to 3.0 K, and the relative humidity varies from 0.7 to 0.9.

this regulation makes the prediction of Q_S under the condition of Fig. 6 better, it is not appropriate for all the conditions. Thus, we have not used the regulated Q_S in the previous discussions.

Figure 7 shows the variation in C_G/C_D under various conditions. These are calculated using the value of Q_S without the abovementioned regulation. The temperature difference $T_w - T_{10}$ in these examples varies from 0.5 to 3.0 K, and RH varies from 70% to 90%. Under the strongest wind conditions ($u_{10} = 28$ m s^{-1}), C_G/C_D increases with increasing temperature difference or decreasing relative humidity. It is interesting to note that in every case, the ratio levels off at approximately 0.7 with winds exceeding 20 m s^{-1}.

4. Conclusions

A boundary layer model over a mature sea was developed for the evaluation of sensible and latent heat fluxes at wind speeds of up to 28 m s^{-1}. To estimate the turbulent stress, we solved the wave boundary layer model of Hara and Belcher (2004). Sea spray effects were incorporated using the parameterization of Fairall et al. (1994). It was confirmed that for weak to moderate winds ($4 \leq u_{10} \leq 18$ m s^{-1}), the drag coefficient and the heat exchange coefficient without sea spray effects are consistent with a bulk algorithm developed using TOGA COARE and HEXOS observations.

The main result of the present study is that while the ratio of the exchange coefficient of total enthalpy to the drag coefficient (C_G/C_D) decreases with increasing wind speed below 20 m s^{-1}, the ratio plateaus at approximately 0.7 for stronger winds ($20 \leq u_{10} \leq 28$ m s^{-1}) under tropical cyclone conditions (wet air blowing over a warm mature sea). It has not been possible to obtain this result using traditional bulk algorithms, which afford a monotonic decrease in C_G/C_D with increasing wind speed. Our result supports the argument of Emanuel (1995a), who showed that the intensity of a tropical cyclone can only be maintained if this ratio remains greater than 0.75 in the strong wind region of intense storms.

The wave boundary layer model adopted here assumes that the perturbations due to interfacial waves reach the inner region depth, which is expressed simply as $z_i = \delta/k$. This expression is applicable for low or high wave ages, but it is not appropriate for intermediate wave ages, at which the inner region depth is thicker and dependent on wave age. The characteristics of flow perturbations differ among these cases, as shown in the previous study of Kihara et al. (2007). Although the wave-age range of intermediate wave age is not large and its effects on the momentum and heat transfer mechanism would be weak, we should confirm the effects of intermediate wave age.

Under tropical cyclones, the local wave state is determined not only by the local wind speed but also by the past wave state; that is, it is not a mature sea state, although the proposed boundary layer model in the present study is developed using wave spectrum under mature sea states. In applying our proposed model to the tropical cyclone conditions, the local wave spectrum should be used instead of the wave spectrum under a mature sea. To incorporate the local wave spectrum, it is necessary to couple our model with a wave model, such as WAVEWATCH III or WAM cycle 4, as carried out in Moon et al. (2004a,b,c).

Acknowledgments. I thank two anonymous referees for their useful comments and suggestions.

REFERENCES

Andreas, E. L, 1990: Time constants for the evolution of sea spray droplets. *Tellus,* **42B,** 481–497.

——, 1992: Sea spray and the turbulent air-sea heat fluxes. *J. Geophys. Res.,* **97,** 11 429–11 441.

——, 1998: A new sea spray generation function for wind speeds up to 32 m s^{-1}. *J. Phys. Oceanogr.,* **28,** 2175–2184.

——, and B. Murphy, 1986: Bulk transfer coefficients for heat and momentum over leads and polynyas. *J. Phys. Oceanogr.,* **16,** 1875–1883.

——, and J. K. DeCosmo, 1999: Sea spray production and influence on air-sea heat and moisture fluxes over the open ocean. *Air-Sea Exchange: Physics, Chemistry and Dynamics,* G. L. Geernaert, Ed., Kluwer Academic, 363–409.

——, and K. A. Emanuel, 2001: Effects of sea spray on tropical cyclone intensity. *J. Atmos. Sci.,* **58,** 3741–3751.

——, and J. K. DeCosmo, 2002: The signature of sea spray in the

HEXOS turbulent heat flux data. *Bound.-Layer Meteor.,* **103,** 303–333.

Belcher, S. E., and J. C. R. Hunt, 1993: Turbulent shear flow over slowly moving waves. *J. Fluid Mech.,* **251,** 109–148.

Charnock, H., 1955: Wind stress on a water surface. *Quart. J. Roy. Meteor. Soc.,* **81,** 639–640.

DeCosmo, J., K. B. Katsaros, S. D. Smith, R. J. Anderson, W. A. Oost, K. Bumke, and H. Chadwick, 1996: Air-sea exchange of water vapor and sensible heat: The Humidity Exchange over the Sea (HEXOS) results. *J. Geophys. Res.,* **101,** 12 001–12 016.

Donelan, M. A., B. K. Haus, N. Reul, W. J. Plant, M. Stiassnie, H. C. Graber, O. B. Brown, and E. S. Saltzman, 2004: On the limiting aerodynamic roughness of the ocean in very strong winds. *Geophys. Res. Lett.,* **31,** L18306, doi:10.1029/2004GL019460.

Elfouhaily, T., B. Chapron, K. Katsaros, and D. Vandemark, 1997: A unified directional spectrum for long and short wind-driven waves. *J. Geophys. Res.,* **102,** 15 781–15 796.

Emanuel, K. A., 1986: An air-sea interaction theory for tropical cyclones. Part I: Steady-state maintenance. *J. Atmos. Sci.,* **43,** 585–604.

——, 1995a: Sensitivity of tropical cyclones to surface exchange coefficients and a revised steady-state model incorporating eye dynamics. *J. Atmos. Sci.,* **52,** 3969–3976.

——, 1995b: The behavior of a simple hurricane model using a convective scheme based on subcloud-layer entropy equilibrium. *J. Atmos. Sci.,* **52,** 3960–3968.

Fairall, C. W., J. D. Kepert, and G. J. Holland, 1994: The effect of sea spray on surface energy transports over the ocean. *Global Atmos. Ocean Syst.,* **2,** 121–142.

——, E. F. Bradley, D. P. Rogers, J. B. Edson, and G. S. Young, 1996: Bulk parameterization of air-sea fluxes for Tropical Ocean-Global Atmosphere Coupled-Ocean Atmosphere Response Experiment. *J. Geophys. Res.,* **101,** 3747–3764.

Hara, T., and S. E. Belcher, 2002: Wind forcing in the equilibrium range of wind-wave spectra. *J. Fluid Mech.,* **470,** 223–245.

——, and ——, 2004: Wind profile and drag coefficient over mature ocean surface wave spectra. *J. Phys. Oceanogr.,* **34,** 2345–2358.

Hasselmann, K., and Coauthors, 1973: Measurements of wind-wave growth and swell decay during the Joint North Sea Wave Project (JONSWAP). *Dtsch. Hydrogh. Z. Suppl. A,* **8,** 1–95.

Janssen, P. S. E. M., 1989: Wave-induced stress and the drag of air flow over sea waves. *J. Phys. Oceanogr.,* **19,** 745–754.

Kepert, J. D., C. W. Fairall, and J.-W. Bao, 1999: Modelling the interaction between the atmospheric boundary layer and evaporating sea spray droplets. *Air-Sea Exchange: Physics, Chemistry and Dynamics,* G. L. Geernaert, Ed., Kluwer Academic, 363–409.

Kihara, N., H. Hanazaki, T. Mizuya, and H. Ueda, 2007: Relationship between the airflow at the critical height and momentum transfer to the traveling waves. *Phys. Fluids,* **19,** 015 102, doi:10.1063/1.2409736.

Kitaigorodskii, S. A., 1973: *The Physics of Air-Sea Interactions*. Keter Press, 273 pp.

Komen, G. J., L. Cavaleri, M. Donelan, K. Hasselmann, S. Hasselmann, and P. A. E. M. Janssen, 1994: *Dynamics and Modeling of Ocean Waves*. Cambridge University Press, 520 pp.

Kondo, J., 1994: *Meteorology of the Water Environment: Water and Heat Balance of the Earth's Surface* (in Japanese). Asakura Shoten Press, 348 pp.

Large, W. G., and S. Pond, 1981: Open ocean momentum flux measurements in moderate to strong winds. *J. Phys. Oceanogr.,* **11,** 324–336.

Lighthill, J., G. Holland, W. Gray, C. Landsea, G. Craig, J. Evans, Y. Kurihara, and C. Guard, 1994: Global climate change and tropical cyclones. *Bull. Amer. Meteor. Soc.,* **75,** 2147–2157.

Liu, W. T., K. B. Katsaros, and J. A. Businger, 1979: Bulk parameterization of air-sea exchanges of heat and water vapor including the molecular constrains at the interface. *J. Atmos. Sci.,* **36,** 1722–1735.

Makin, V. K., 1999: A note on wind speed and sea state dependence of the heat exchange coefficient. *Bound.-Layer Meteor.,* **91,** 127–134.

——, and C. Mastenbroek, 1996: Impact of waves on air-sea exchange of sensible heat and momentum. *Bound.-Layer Meteor.,* **79,** 301–306.

——, and V. N. Kudryavtsev, 1999: Coupled sea surface-atmosphere model 1. Wind over waves coupling. *J. Geophys. Res.,* **104,** 7613–7623.

Moon, I.-J., T. Hara, I. Ginis, S. E. Belcher, and H. Tolman, 2004a: Effect of surface waves on air–sea momentum exchange. Part I: Effect of mature and growing seas. *J. Atmos. Sci.,* **61,** 2321–2333.

——, I. Ginis, and T. Hara, 2004b: Effect of surface waves on air–sea momentum exchange. Part II: Behavior of drag coefficient under tropical cyclones. *J. Atmos. Sci.,* **61,** 2334–2348.

——, ——, and ——, 2004c: Effect of surface waves on Charnock coefficient under tropical cyclones. *Geophys. Res. Lett.,* **31,** L20302, doi:10.1029/2004GL020988.

——, ——, ——, and B. Thomas, 2007: Physics-based parameterization of air–sea momentum flux at high wind speeds and its impact on hurricane intensity predictions. *Mon. Wea. Rev.,* **135,** 2869–2878.

Phillips, O. M., 1977: *The Dynamics of the Upper Ocean*. 2nd ed. Cambridge University Press, 336 pp.

——, 1985: Spectral and statistical properties of the equilibrium range in the wind-generated gravity waves. *J. Fluid Mech.,* **156,** 505–531.

Pierson, W. J., and L. Moskowitz, 1964: A proposed spectral form for fully developed wind sea based on the similarity theory of S. A. Kitaigorodskii. *J. Geophys. Res.,* **69,** 5181–5190.

Powell, M. D., P. J. Vickery, and T. A. Reinhold, 2003: Reduced drag coefficient for high wind speeds in tropical cyclones. *Nature,* **422,** 279–283.

Rotunno, R., and K. A. Emanuel, 1987: An air–sea interaction theory for tropical cyclones. Part II. *J. Atmos. Sci.,* **44,** 542–561.

Tolman, H. L., 2002: User manual and system documentation of WAVEWATCH-III, version 2.22. NOAA/NWS/NCEP/OMB Tech. Note 222, 133 pp.

Wang, Y., J. D. Kepert, and J. Holland, 2001: The effect of sea spray evaporation on tropical cyclone boundary layer structure and intensity. *Mon. Wea. Rev.,* **129,** 2481–2500.

Wu, J., 1973: Spray in the atmospheric surface layer: Laboratory study. *J. Geophys. Res.,* **78,** 511–519.

Zeng, X., M. Zhao, and R. E. Dickinson, 1998: Intercomparizon of bulk aerodynamic algorithms for the computation of sea surface fluxes using TOGA COARE and TAO data. *J. Climate,* **11,** 2628–2644.